

Color change characteristics of two shear-sensitive liquid crystal mixtures (BCN/192, BN/R50C) and their application in surface shear stress measurements

ZHAO JiSong^{1,2*}, SCHOLZ Peter² & GU LiangXian¹

¹ School of Astronautics, Northwestern Polytechnical University, Xi'an 710072, China;

² Institute of Fluid Mechanics, TU Braunschweig, Braunschweig 38106, Germany

Received April 10, 2011; accepted June 3, 2011

A previously determined surface shear stress measurement technique using shear-sensitive liquid crystal (SSLC) coating is extended for use in wind tunnel-like conditions. Simple and common everyday equipment is used in the measurement; in particular a tungsten halogen light bulb provides illumination. The color change characteristics of two SSLC mixtures, BCN192 and BN/R50C, are investigated. BCN/192 is found sensitive to both magnitude and direction of the shear stress at different shear stress levels with little noise, and is suitable for surface shear stress distribution measurements. The spatial shear stress vector distribution beneath a tangential jet is obtained using BCN/192, although the magnitude is not fully calibrated. BN/R50C is found to be sensitive to shear stress magnitude, but only slightly sensitive to shear stress direction at both low and high levels. Moreover, jumps in the reflected hue are found when the viewing orientation is perpendicular to the shear stress direction. These characteristics render the use of BN/R50C for surface shear stress measurement difficult.

shear-sensitive liquid crystals, surface shear stress measurement, tangential jet flow

Citation: Zhao J S, Scholz P, Gu L X. Color change characteristics of two shear-sensitive liquid crystal mixtures (BCN/192, BN/R50C) and their application in surface shear stress measurements. *Chinese Sci Bull*, 2011, 56: 2897–2905, doi: 10.1007/s11434-011-4673-y

Wall shear stress is an important fluid parameter. In aerodynamics research, much valuable information can be gained from visualizing and measuring shear stress patterns on solid surfaces. Frictional forces generated by gases or liquids flowing over these surfaces can significantly influence the performance of aircraft, ships, or surface-transport vehicles. Internal frictional forces, such as those caused by air compression through a jet engine or blood flow through an artificial heart chamber, also affect aerodynamic or mechanical performance. However, wall shear stress measurements remain very challenging. In the past, shear stress was measured by varying mechanical or electrical means, such as mechanical balances or intrusive probes and sensors [1,2]. Those methods typically disturbed the flow and measured point-wise. Any means to measure shear stress efficiently

with a high spatial resolution would be interesting for the assessment of fluidic vortex generator jets or other flow control devices. Recently, Reda et al. [3] studied a method for measuring the shear stress distribution with the use of a shear-sensitive liquid crystal (SSLC) coating sprayed over a target surface. Such coatings produce a color spectrum when illuminated by white light. The color is known to vary with the shear stress direction and magnitude and the angles of observation and illumination. The color changing properties of these coatings are due to their helical structure. For molecular studies of similar coatings, refer to Wei et al. [4] and Liu et al. [5]. When the color is calibrated against such parameters, the visualized color image can be converted into a shear stress vector field over the surface. The power of the technique was demonstrated by the measurement of the shear stress vector fields beneath a wall tangential jet [3] and an inclined impinging jet [6]. The accuracies were

*Corresponding author (email: zhaojisongjinling@163.com)

found to be equivalent to conventional point measurement techniques.

Previously, Fujisawa et al. [7] studied instantaneous surface shear stress distributions from measurements using an SSLC coating. Two synchronized cameras were placed side by side. The relative hue of each camera was calibrated with respect to the surface shear stress direction and magnitude, which can then be determined by minimizing the interpolation error between the two sets of calibration curves. The technique was applied to the measurement of shear stress distributions around a circular cylinder on a surface. In other research [8], Nakano et al. extended this technique to wind tunnel studies. Instantaneous shear stress coefficients over the test surface around a surface mounted circular cylinder at two different instants were measured. In their latest research [9], Nakano et al. used this technique to measure wall shear stress distributions over curved surfaces (NACA0018 airfoil). In contrast to earlier research, the relative hue of each camera was calibrated with respect to shear stress directions, shear stress magnitudes, and observation angles. Although the results of liquid crystal (LC) coating technique agreed with that of near-wall particle image velocimetry (PIV), this coating technique showed larger uncertainties than the PIV measurement, both for measurements on a flat plate and on the NACA0018 airfoil. The uncertainties were attributed to the calibration error, the observation and illumination angle error, and the lower sensitivity at higher shear stress of the LC used.

In earlier research [10], Reda et al. compared the accuracy of different approaches to obtain the shear stress vector under normal illumination. The two-perspective approach was found to be less accurate. Use of five or more observations and Gaussian curve fitting yielded measured vector orientations within $\pm 1^\circ$ and measured vector magnitudes within $\pm 5\%$ of control measurements; discrepancies in measured magnitudes as high as 22% were found, with corresponding discrepancies in orientation as large as 4° for the two-perspective approach. This is easy to understand because the curve fitting used five or more observations while the two-perspective approach used only two observations. However, in current research, the two-perspective approach can be extended to three-dimensional measurements, while the Gaussian curve fitting approach is confined to planar measurements.

The research of Reda et al. and Fujisawa et al. were conducted in carefully-arranged conditions. There are some problems in extending the measurement techniques to wind tunnel studies. In Reda et al.'s research, a special illumination source (NAC Visual Systems HMI-1200) was used to supply normal white light. This lighting is not easily accessible to other researchers. Moreover, a new LC coating was applied for each view, making measurements complicated and expensive. In the research of Fujisawa et al., the calibration methodology required rotation of the test section, which made the calibration facility rather complicated. In

addition, changes in perspective and illumination angles across the target area were not considered, and the measurement was confined to a small area of about 2.5 cm by 2.5 cm. Although the illumination angle was considered in their latest research, the measurement was still confined to an area 3 cm \times 3 cm because of changes in perspective across the target area. The purpose of the present paper is to extend the surface shear stress measurement technique determined by Reda et al. to wind tunnel studies, with all the special facilities replaced by common ones, and then to investigate the color change characteristics of two kinds of SSLC mixtures, BCN192 and BN/R50C.

1 Experimental apparatus

1.1 General description

The experiments were conducted on the test plate of a low-speed wind tunnel at the Institut für Strömungsmechanik at the Technische Universität Braunschweig, Braunschweig, Germany. The maximum velocity within the wind tunnel is 30 m/s. The tunnel has a test plate of 758 mm by 420 mm with an oblate elliptical leading edge. To enhance the quality of the color change in an LC coating, a black anodized aluminum 'plug' of 100 mm by 100 mm was mounted in the center of the test plate. The test plate is used to define the physical x - y plane, and the flat plate centerline (also the 'plug' centerline) is used to define the $\phi=0^\circ$ reference. A rotating arm is built so that the above-plane view angle (denoted as α) is constant when recording the coating color change at different circumferential view angles (also called the in-plane view angle and denoted as ϕ). Figure 1 shows the wind tunnel with the test plate and the rotating arm. The rotating arm can be rotated through 180° from -90° to 90° . The above-plane view angle is fixed during the experiment.

1.2 Setting of above-plane view angle

The above-plane view angle α was set to a constant with the help of the rotating arm. However, the above-plane view angle should be optimized to maximize the color change signal for the LC mixture in use and the shear stress field imposed upon it. A comparison of hue- ϕ curves at different above-plane view angles is given in Figure 2. The comparison experiment was conducted on the flat plate at a wind-tunnel outlet velocity of 23.0 m/s. The hue of each view corresponds to the average value across an area of 6 cm by 6 cm. It is clear to find that the coating is more sensitive to a smaller above-plane view angle. However, the above-plane view angle should not be set too small in this research otherwise the camera would be blocked by the upper side of the wind tunnel mouth. Too small above-plane view angle would also induce considerable image geometry transformation error in latter analysis. In later experiments, the camera above-plane view angle was set to about 28° .

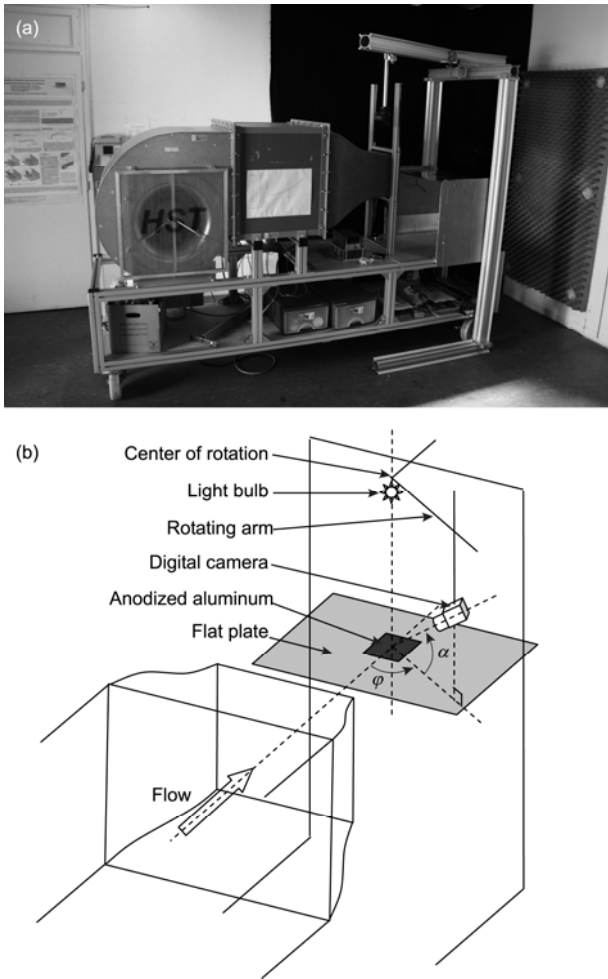


Figure 1 (a) Wind tunnel with the test plate and the rotating arm; (b) schematic diagram of the experimental set-up.

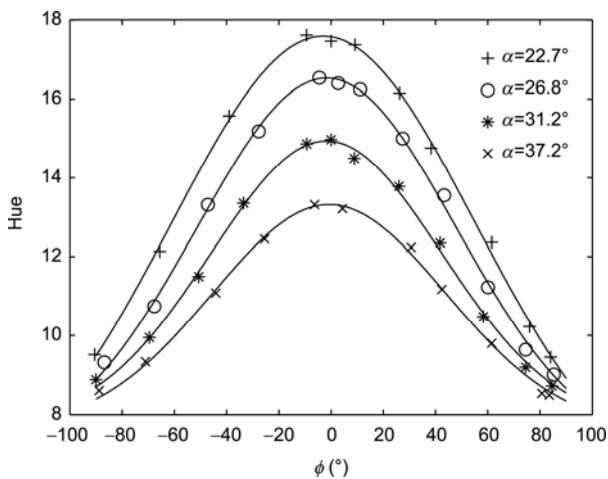


Figure 2 Hue- ϕ curve at different above-plane view angles ($u = 23.0$ m/s).

1.3 Illumination source

In extending the Reda et al.'s research to wind tunnel measurements, the most difficult aspect was the special lighting

needed to supply normal white light. Unfortunately, such a light source is complicated and currently not commercially available. In our experimental setup, we looked for a simple light source as a substitute. A wind tunnel experiment was designed to verify whether the light source was suitable in measurements. As illustrated in Figure 3, the light source was placed at a height of 86 cm above the center of a flat plate illuminating an area of interest of size 6 cm by 6 cm. The experiment was conducted at a wind tunnel velocity of 19.9 m/s. The flow was generally the same across the square and so the hue- ϕ curve at the center, left, top, right and down (viewing downstream) of the square should coincide with each other if the light directions were sufficiently parallel.

A number of different light sources were tested in our preliminary study. It was found that extended light was better than focused light because the latter always had some halation. However, none of these provided suitable lighting for measurement taking. Typical hue- ϕ curves at the five locations are given in Figure 4, which were obtained under the illumination of a 40 W incandescent lamp with a lampshade diameter of about 15 cm. The hue was the average value of a window size of 1 cm by 1 cm at each location. The curves do not coincide with each other due to perspective differences. It is easy to compute that the illumination angle varies about 14° among the five locations. Taking into consideration Figures 3 and 4, we conclude that oblique illumination causes the hue- ϕ curve to shift towards the direction of light and become a little symmetrical about the light plane, in agreement with Reda et al. [11].

Because none of the many lights we tested were suitable, we decided to build a light source ourselves. We constructed a 20 W small tungsten halogen bulb with a thin aluminum cap for shielding attached to the top to reduce the reflection

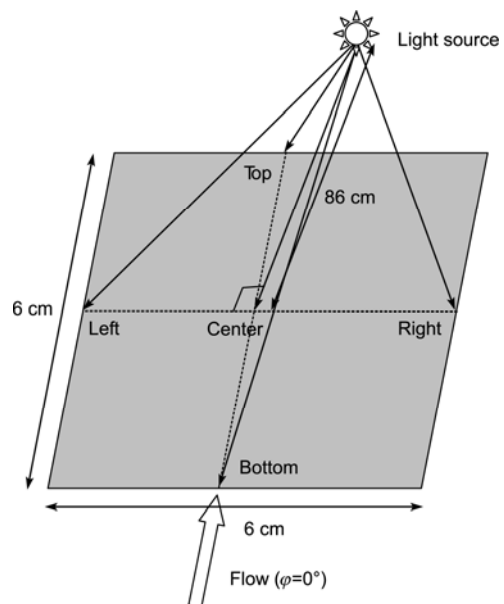


Figure 3 Illumination angle differences across the five locations.

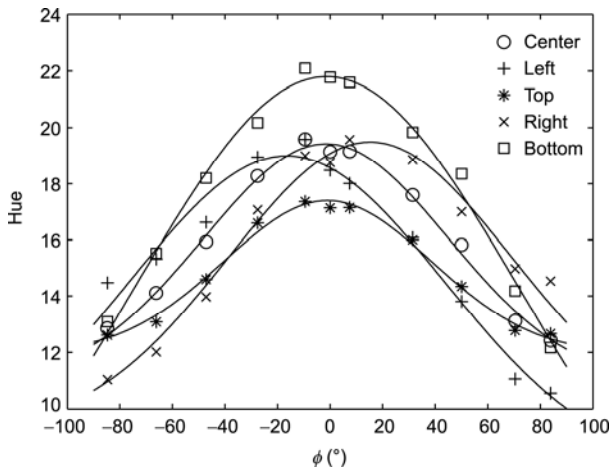


Figure 4 Hue- ϕ curves at the five locations ($u = 19.9$ m/s, incandescent lamp illumination).

of the ceiling and experimental shelves. The maximal size of the bulb was about 5 mm, so the light angle differences to each of the five locations was less than 4.3° . This difference could be further reduced by increasing the height of the bulb above the plate. Figure 5 gives the hue- ϕ curves at the same five locations under the illumination of our light bulb. The five curves coincide well with each other. The maximum hue of each curve varies from 18.7 to 19.9 and the symmetry angle varies from -2.9° to 3.1° . The slight discrepancies were mainly due to uneven coating thickness. One drawback of this self-made light source was its low intensity. Exposure times were about 1 s, even though the lens aperture was set to the maximum value, and therefore did not enable instantaneous flow measurements to be taken.

1.4 Image facility and color calibration

A frame grabber and video camera was used in the work of

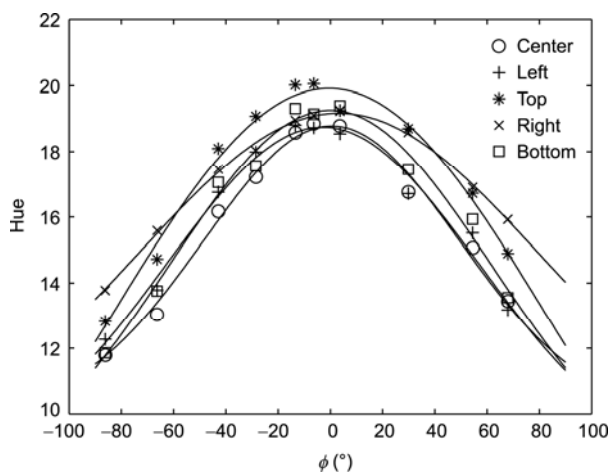


Figure 5 Hue- ϕ curves at the five locations ($u = 19.9$ m/s, illuminated with a small light bulb).

Reda et al., and the color was calibrated with the standard Macbeth color checker. In this investigation, images were recorded with a Canon EOS 400D color digital camera (made in China). The 'Manual' shot mode was used with the lens aperture set to $F = 5.6$ and the exposure time set to $T = 1$ s. A page of white A4 printing paper was used to set the customized white balance. There is no need to calibrate the color in standard color space, thus a self-made Macbeth color checker which was generated on a computer and printed on high quality color printer was used to calibrate the color [12]. The color calibration was found to be helpful in reducing random noises and was performed any time the imaging system (illumination source or digital camera) was changed to standardize color measurements in an even space.

2 SSLC and technique evaluation

The SSLC mixtures used in this project were supplied by LCR Hallcrest (U.K.). There are three standard mixtures, as listed in Table 1. The first two (BCN/192 and BN/R50C) were analyzed as part of the present research. BCN/192 was used for surface shear stress measurements by Reda et al. [3,6], while BN/R50C was used only for flow visualization and not for surface shear stress measurements as seen in [13–15].

Also listed in Table 1 are the relative viscosity and the flow speed working range of each LC mixture; all values are different. However, these parameters are not necessarily the ones that will provide assistance in determining which crystal to use for a particular application. A low viscosity does not mean that it will be the most useful at low velocity or shear stress [16]. As will be shown later, both BCN/192 and BN/R50C tend to flow, but neither was blown away at a jet velocity of about 120 m/s. Alternatively, flow speed is not a good parameter to quantify shear stress, because the shear stress can vary widely for fixed flow velocity.

The liquid crystals were uniformly sprayed onto the aluminum 'plug' with an air brush after being mixed with acetone (about 10% LC in volume). The acetone evaporated quickly after spraying, leaving a red LC coating of on the test surface. The thickness of the coating is about $10 \mu\text{m}$ (based on mass conservation and estimated spray losses). It was found that crystal LC coating that is too thin gave little color change whereas one too thick tended to flow.

Table 1 Liquid crystal characteristics

Type	Relative viscosity at 30°C	Flow speed working range (m/s)	
BN/R50C	Chiral-nematic	1	<30
BCN/192	Mixed	4	30–70
CN/R3	Cholesteric	15	75–200

3 Transformation of color image to shear stress distribution

To analyze the color change in LC coatings in physical coordinates, we performed a perspective transformation on each image to map the image coordinates to the physical coordinates on the test surface. Exterior parameters for the camera were determined for each image using four reference marks that were machined at the vertices of the square around the ‘plug’.

For color measurements, it is more useful to represent the signal in terms of hue, saturation, and intensity (HSI) rather than red, green and blue (RGB). Only the hue images were used for further analysis. Spatial filters over the 10×10 pixel neighborhood were applied to all the hue images to reduce the standard deviation of the hue variation while preserving the hue gradient. According to the second trichromatic system discussed in [17], the hue can be calculate from

$$h = \tan^{-1} \left(\frac{\sqrt{3} \cdot (G - B)}{2R - G - B} \right) + \theta, \quad \theta = \begin{cases} 0 & 2R \geq G + B, \\ \pi & 2R < G + B, \end{cases} \quad (1)$$

where h is the hue, $h \in [-90^\circ, 270^\circ)$; R , G and B are the three primary colors, red, green and blue, respectively. In this trichromatic system, red ($R=1, G=0, B=0$) is placed at 0° , green ($R=0, G=1, B=0$) is placed at 120° , and blue ($R=0, G=0, B=1$) is placed at 240° .

Read et al. [18] found that under normal illumination and fixed above-plane viewing angle, the maximum hue of SSLC coating for a given shear stress magnitude was measured when the shear vector was aligned with, and directed away from, the observer; changes in circumferential angle either side of the vector aligned position resulted in symmetric decrease in hue. The hue- ϕ change could be well fit by a Gaussian curve between -90° and $+90^\circ$:

$$h(\phi) = (h(\phi_\tau) - h_{VN}) \cdot \exp \left[- \left(\frac{\phi - \phi_\tau}{\sigma} \right)^2 \right] + h_{VN}, \quad (2)$$

where h_{VN} is the hue observed for an in-plane view angle normal to the shear vector (i.e. $|\phi_\tau - \phi| = 90^\circ$), σ is the standard deviation of the Gaussian distribution, and ϕ_τ and $h(\phi_\tau)$ are the orientation of the shear stress vector and the hue observed when ϕ is aligned with the vector (referred to as vector-aligned hue), respectively.

A calibration curve of vector-aligned hue vs. shear stress magnitude is required for the specific arrangement wherein the calibration shear stress vector is aligned with and directed away from the camera. In Reda et al.’s research, fringe-imaging (oil-drop) skin friction technique, was used for this purpose. In our research, the friction formula over a flat plate was used to calibrate the vector-aligned hue vs. shear stress magnitude. A piece of aluminum tape cut in a zigzag pattern with pinking shears was applied onto the flat

plate, at about 6 cm from the zigzag to the leading edge of the plate to generate a turbulence boundary layer. A reasonable local turbulent friction over the flat plate is

$$\tau = \frac{1}{2} \rho u^2 \cdot c_f, \quad c_f = 0.0592 \cdot Re^{-\frac{1}{5}}, \quad Re = \rho ul / \mu, \quad (3)$$

where ρ is the air density; u is the wind tunnel velocity; l is the reference length, measured from the leading edge of the flat plate; μ is the dynamic viscosity, $\mu = 17.9 \times 10^{-6}$ Pa s; and Re is the Reynolds number.

The camera in-plane view angle $\phi = 0^\circ$ served as the angular reference point. The wind tunnel outlet velocity could be varied, as did the shear stress magnitude. The vector-aligned hue vs. shear stress magnitude calibration curve for BN/R50C is shown in Figure 6.

Three example datasets of hue vs. ϕ are shown in Figure 7. The data were taken with settings $u = 100, v = 300, u = 124, v = 300$, and $u = 136, v = 300$ corresponding to the image coordinates depicted in Section 4. The ϕ corresponding

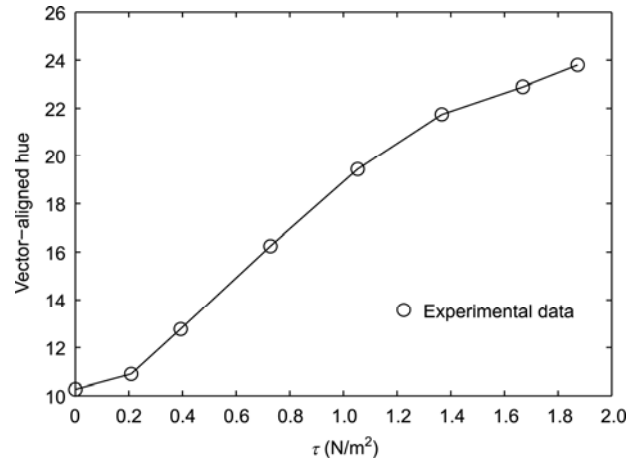


Figure 6 Vector-aligned hue vs. shear stress magnitude calibration curve (BN/R50C).

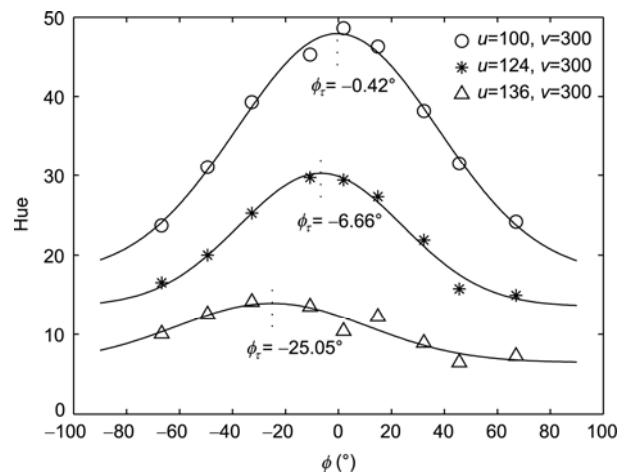


Figure 7 Hue- ϕ curves for two different shear stress vectors.

to the maximum of the curves determine the vector orientation ϕ_r . The vector-aligned hue value was then converted to a shear stress magnitude via a vector-aligned hue vs. shear stress magnitude calibration curve. The curve fitting procedure was repeated at each pixel within the test area, and all the shear stress vectors over the test surface could be obtained.

4 Color change characteristics of BCN/192

The comparison studies of BCN/192 and BN/R50C were not actually conducted in a wind tunnel flow. Instead, a jet nozzle was affixed to the flat plate, as shown in Figure 8, supplying dry filtered air at room temperature from a pressurized gas tank connected to a compressor. The jet nozzle was a circular copper tube of outer diameter 12 mm, and inner diameter 3.8 mm, with a blunt tip. A line drawn on the flat plate centerline allowed for an accurate alignment of the jet centerline and the plate centerline. The jet was affixed to the flat plate 1 cm away from the 'plug' front edge, and inclined at an angle of about 2.5° relative to the plane of the 'plug'. A pressure regulator controlled the pressure at a fixed 0.17 bar, with a corresponding jet centerline exit velocity of 120 m/s. The regulator was an open-loop controller and thus the jet flow was very unsteady, although care was taken to make sure the jet flow did not change much during the experiment.

The surface shear stress vector field beneath a tangential jet was measured by Reda et al. [3]. In that work, a new LC coating was applied for each view. In our preliminary study [19], we found a saturation of LC coating color change with time. In the present research, measurements were taken after the coatings produced a steady color and thus only one coating was used for all views required for the Gaussian curve fittings. Three raw images at different in-plane view angles are given in Figure 9 to demonstrate the color change

in BCN/192. The coordinates are given in pixel units. The images were rotated into the normal view and the unwanted portions were cropped. The resolution was set so that 1 mm in physical coordinates corresponds to five pixels in the image plane. The image corresponding to $\phi = 2.0^\circ$ is symmetric about the centerline ($u = 100$) due to camera alignment with the plate centerline and the symmetry of the shear vector field itself (magnitudes and directions) relative to the plate centerline. The $\phi = -66.7^\circ$ and $\phi = 67.1^\circ$ images are essentially mirror images, but each appears slightly asymmetric relative to the centerline. This asymmetry is a direct result of the dual dependence of color change response of the coating on shear magnitude and its direction relative to the observer: both quantities vary across the jet-induced shear field.

Several points along the plate centerline were chosen to represent different shear stress levels. The points selected were $u = 100, v = 1, 100, 150, 200, 300$ and 400 in the image coordinates marked in Figure 9. The hue- ϕ curves at these points are plotted in Figure 10. Note that noise were slight even though the curves were obtained for a single measurement, i.e. only one image was used for each ϕ view. Noise

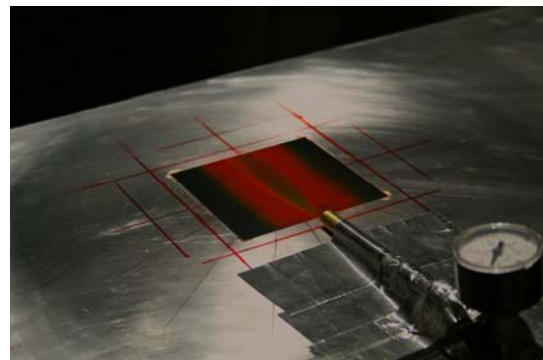


Figure 8 Overview of air jet attached to the flat plate.

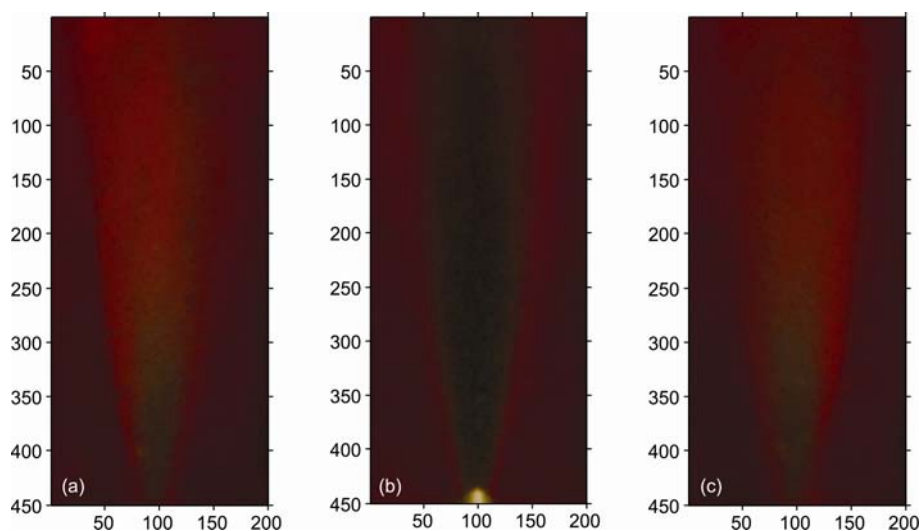


Figure 9 Color changes in BCN/192 at different in-plane view angles. (a) $\phi = -66.7^\circ$; (b) $\phi = 2.0^\circ$; (c) $\phi = 67.1^\circ$.

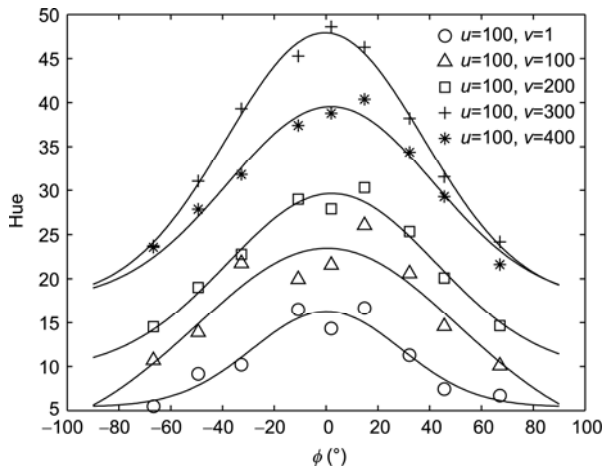


Figure 10 Hue versus in-plane view angle (9 images, Gaussian curve fit, BCN/192).

could be further reduced if a time-average was performed during acquisition. The maximum of the curves in Figure 10 are generally at $\phi=0^\circ$ because the shear stresses along the plate centerline are of $\phi=0^\circ$ orientation.

The curve fitting procedure described in Section 3 was repeated at each pixel of the test plate, and all the shear stress vectors over the test surface could be obtained. Unfortunately no calibration curve was obtained for BCN/192, even though we obtained a calibration curve for BN/R50C as given in Figure 6. Figure 11 shows a representation of the wall-jet-induced shear stress vector distribution measured with a BCN/192 coating. The vector field was an average of five measurements. The vectors were computed every four pixels along several profiles. Because no hue vs. shear stress calibration was obtained for BCN/192, the vector length was vector-aligned hue but not shear stress magnitude. However, since the relationship between shear stress magnitude and vector-aligned hue is nearly linear (see Figure 6 for BN/R50C), a relative comparison would be possible (e.g. relative to maximum τ , or maximum vector-aligned hue, respectively).

5 Color change characteristics of BN/R50C

The color change characteristics of BN/R50C are investigated in this section. A similar procedure and analysis were performed as for BCN/192. Three raw images at different in-plane view angles are given in Figure 12.

The hue- ϕ curves at points along the centerline are given in Figure 13 from which it can be seen that the hue is found to be sensitive to shear stress magnitude, but only slightly sensitive to in-plane view angle ϕ , irrespective of whether the shear stress is low or high, although BN/R50C has a low viscosity. Considerable noise appears in each curve and some jumps in data near the $\phi=\pm 90^\circ$ locations with exception at the highest shear stress level. These problems make

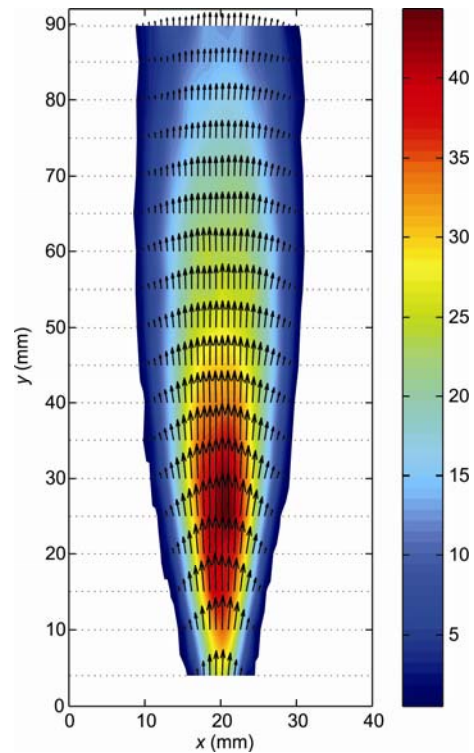


Figure 11 Surface shear stress vector field beneath a jet flow (color contours vector-aligned hue).

the surface shear stress measurement using BN/R50C seem difficult.

We explain the ‘strange’ jumps as follows. As BN/R50C has a lower viscosity, it tends to be blown into strips along the flow direction. Due to these strips, the intensities of the reflected light at $\phi=\pm 90^\circ$ views are high, whereas the intensity of the reflected light at $\phi=0^\circ$ is low. The high light intensity requires less exposure, while the low light intensity requires more. In the ‘Manual’ mode, the camera lens aperture and exposure time are fixed. If the $\phi=0^\circ$ image is properly exposed, the $\phi=\pm 90^\circ$ images will be over exposed and vice versa. Over-exposing increases the hue value, and under-exposing reduces the hue value. For a complicated flow field, ensuring that every pixel is exposed properly is rather difficult.

Comparing the experimental results of Sections 4 and 5, BCN/192 shows ‘good’ hue- ϕ characteristics at both low and high shear stress levels although it has a higher viscosity, and is suitable for surface shear stress vector measurements. In contrast, BN/R50C does not exhibit ‘good’ hue- ϕ characteristics, and is not suitable for surface shear stress vector unless a new methodology or a better understanding of the behavior of SSLCs is developed.

6 Conclusions

The surface shear stress measurement technique determined

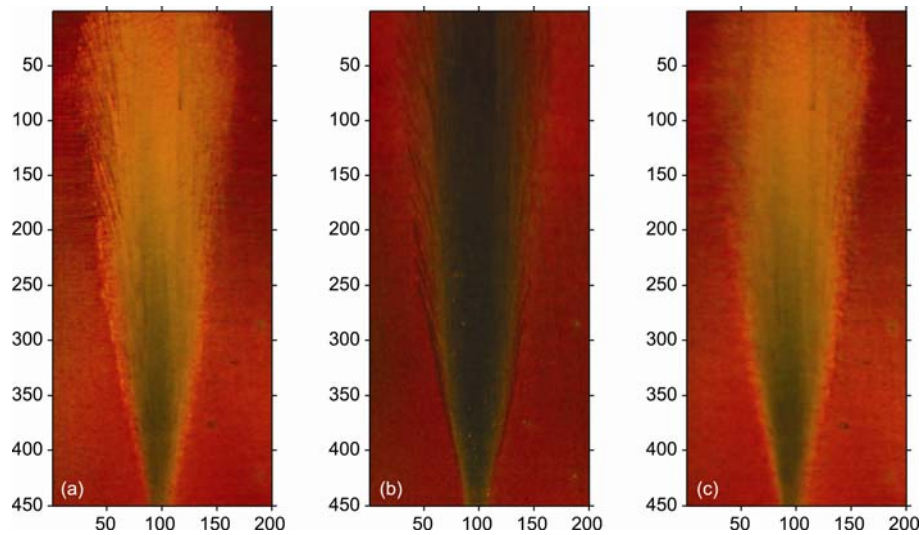


Figure 12 Color changes in BN/R50C at different in-plane view angles. (a) $\phi = -83.0^\circ$; (b) $\phi = 1.7^\circ$; (c) $\phi = 84.8^\circ$.

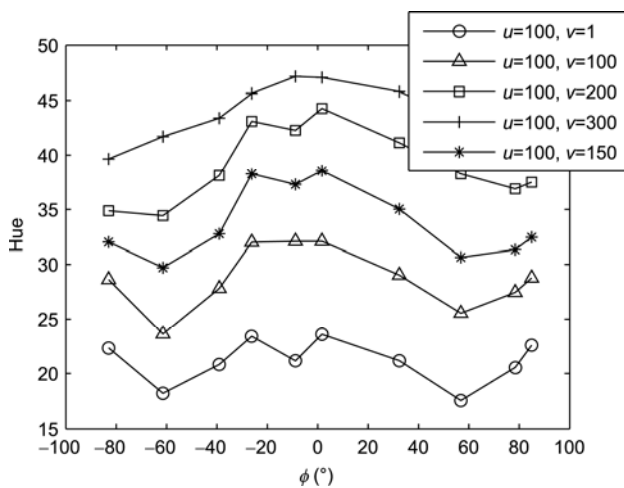


Figure 13 Hue- ϕ curves at different shear stress levels (BN/R50C).

by Reda et al. [3,6] was extended to wind tunnel studies. Our experiments used only simple and common everyday equipment; in particular a small tungsten halogen bulb served as illumination. Although the present current measurements were not conducted in a wind tunnel flow, it is very easy to do so. The color change characteristics of two shear sensitive liquid crystal mixtures, BCN192 and BN/R50C, were investigated. BCN/192 was found sensitive to both shear stress magnitude and direction, and showed 'good' hue- ϕ characteristics with little noise at a level suitable for surface shear stress distribution measurements. Spatial shear stress vector distribution beneath a tangential jet was obtained using BCN/192, although the magnitude was not fully calibrated. BN/R50C was found sensitive to shear stress magnitude, but only slightly sensitive to shear stress direction, no matter whether the shear stress was low or high. In addition, considerable noise was present in the hue- ϕ curves, and a jump in hue in the views near $\phi = \pm 90^\circ$. Meas-

urements of surface shear stress using BN/R50C would be problematic. The potential demonstrated in this study warrants further research that will focus on extending the technique to actual wind tunnel measurements, calibrating the vector-aligned hue vs. shear stress magnitude and reducing noise (e.g. using some high-frequency imaging to perform time averaging).

This work was supported by the Doctorate Creation Foundation of North-western Polytechnical University (CX200902).

- 1 Naughton J W, Sheplak M. Modern developments in shear-stress measurement. *Prog Aerosp Sci*, 2002, 38: 515–570
- 2 Haritonidis J H. The measurement of wall shear stress. *Adv Fluid Mech Meas*, 1989, 45: 229–261
- 3 Reda D C, Wilder M C, Farina D J, et al. New methodology for the measurement of surface shear-stress vector distributions. *AIAA J*, 1997, 35: 608–614
- 4 Wei X L, Yin B L, Sun D Z, et al. Research on colored lyotropic liquid crystals. *Chinese Sci Bull*, 2005, 50: 1586–1591
- 5 Liu G Z, Xia D L, Yang W J, et al. The surface rubbing effect on morphologies of LC droplets and electro-optic properties of flexible PDLC films. *Sci China Ser B-Chem*, 2009, 52: 2329–2335
- 6 Reda D C, Wilder M C, Mehta R, et al. Measurement of continuous pressure and shear distributions using coating and imaging techniques. *AIAA J*, 1998, 36: 895–859
- 7 Fujisawa N, Aoyama A, Kosaka S. Measurement of shear-stress distribution over a surface by liquid-crystal coating. *Meas Sci Tech*, 2003, 14: 1655–1661
- 8 Nakano T, Fujisawa N. Wind tunnel testing of shear-stress measurement by liquid-crystal coating. *J Visual*, 2006, 9: 135–136
- 9 Fujisawa N, Oguma Y, Nakano T. Measurements of wall-shear-stress distribution on a NACA0018 airfoil by liquid-crystal coating and near-wall particle image velocimetry (PIV). *Meas Sci Tech*, 2009, 20: 1–10
- 10 Reda D C, Muratore J J Jr. A new technique for the measurement of surface shear stress vectors using liquid crystal coatings. *AIAA*, 1994, 94-0729
- 11 Reda D C, Muratore J J Jr, Heineck J T. Time and flow direction responses of shear-stress-sensitive liquid crystal coatings. *AIAA J*, 1994: 32: 693–700
- 12 Pascale D. RGB Coordinates of the Macbeth color checker. The

- BabelColor Company Technical Report, 2006
- 13 Zante D E V, Okiishi T H. Visualization of boundary-layer development on turbomachine blades with liquid crystals. Final Technical Report. NASA Grant NAG 3-917, 1991
 - 14 Chong T P, Zhong S, Hodson H P. Visualization of turbulent wedges under favorable pressure gradients using shear sensitive and temperature-sensitive liquid crystals. *Ann New York Acad Sci*, 2003, 972: 95–102
 - 15 Zhong S. Detection of flow separation and reattachment using shear-sensitive liquid crystals. *Exp Fluids*, 2002, 32: 667–673
 - 16 Savory E, Sykes D M, Toy N. Visualisation of transition on an axisymmetric body using shear sensitive liquid crystals. *Opt Diag Eng*, 2000, 4: 16–25
 - 17 Hay J L, Hollingsworth D K. A comparison of trichromic systems for use in the calibration of polymer-dispersed thermochromic liquid crystals. *Exp Thermal Fluid Sci*, 1996, 12: 1–12
 - 18 Reda D C, Muratore J J Jr. Measurement of surface shear stress vectors using liquid crystal coatings. *AIAA J*, 1994, 32: 1576–1582
 - 19 Zhao J S, Scholtz P. Development of wall shear stress measurement technique using liquid crystal coatings. Report of Visiting Research. Braunschweig. Institute of Fluid Mechanics, TU Braunschweig, Germany, 2010

Open Access This article is distributed under the terms of the Creative Commons Attribution License which permits any use, distribution, and reproduction in any medium, provided the original author(s) and source are credited.